Lateral Distribution of Cholesterol in Dioleoylphosphatidylcholine Lipid Bilayers: Cholesterol-Phospholipid Interactions at High Cholesterol Limit

Amanda Parker, Keith Miles, Kwan Hon Cheng, and Juyang Huang
Department of Physics, Texas Tech University, Lubbock, Texas 79409

ABSTRACT Lateral organization of cholesterol in dioleoyl-phosphatidylcholine (DOPC) lipid bilayers at high cholesterol concentration (>45 mol%) was investigated using steady-state fluorescence anisotropy and fluorescent resonance energy transfer techniques. The recently devised Low Temperature Trap method was used to prepare compositionally uniform cholesterol/DOPC liposomes to avoid the problem of lipid demixing. The fluorescence anisotropy of diphenylhexatrience chain-labeled phosphatidylcholine (DPH-PC) in these liposomes exhibited local maxima at cholesterol mol fractions of 0.50 and 0.57, and a sharp drop at 0.67. For the liposomes labeled with both dehydroergosterol and DPH-PC, the fluorescent resonance energy transfer efficiency from dehydroergosterol to DPH-PC displayed a steep jump at cholesterol mol fraction of 0.5, and dips at 0.57 and 0.68. These results indicate the presence of highly ordered cholesterol regular distribution domains at those observed critical compositions. The observed critical mol fraction at 0.67 agreed favorably with the solubility limit of cholesterol in DOPC bilayers as independently measured by light scattering and optical microscopy. The regular distribution at 0.57 was previously predicted from a Monte Carlo simulation based on the Umbrella model. The results strongly support the hypothesis that the primary requirement for cholesterol-phospholipid mixing is that the polar phospholipid headgroups need to cover the nonpolar body of cholesterol to avoid the exposure of cholesterol to water.

INTRODUCTION

Cholesterol is a major constituent of the mammalian plasma membranes. It has been shown that cholesterol has a remarkable ability to induce domain formation in lipid membranes. For example, in dipalmitoyl-phosphatidylcholine (di16:0PC) lipid bilayers at room temperature, cholesterol induces the coexistence of a liquid disordered phase (l_d) with low cholesterol content and a liquid order phase (l_o) with high cholesterol content (Ipsen et al., 1987; Vist and Davis, 1990). In addition, microdomains in the plasma membranes of animal cells known as ''lipid rafts,'' which are rich in cholesterol, sphingolipids, and certain membrane proteins, are thought to be involved in regulating cell functions, such as signal transduction, lipid trafficking, and protein function (Simons and Ikonen, 1997, 2000; Brown and London, 1998, 2000; Field et al., 1997). Similar cholesterol-rich ''raft domains'' have been reproduced on synthetic liposomes as well as planar supported lipid bilayers containing equal molar of unsaturated phosphatidylcholine (PC), sphingomyelin (SM), and cholesterol (Xu and London, 2000; Wang et al., 2000; Dietrich et al., 2001; Samsonov et al., 2001; Gandhavadi et al., 2002). Furthermore, in some mixtures of fluid-phase phospholipids and cholesterol, evidences suggest that cholesterol molecules can form regular distribution domains (e.g., hexagonal or centered rectangular pattern superlattices) to maximize the cholesterol-cholesterol separation (Chong, 1994; Virtanen et. al., 1995; Liu et al., 1997; Wang et al., 2002; Cannon et al., 2003).

Because the domain formations are driven by molecular interactions, a comprehensive understanding of cholesterol-lipid interaction is needed to understand the mechanisms of cholesterol-induced domain formation under various conditions. A good model should identify the key interactions, and be able to explain a wide range of experimental results, or even predict new phenomena. In this study, cholesterol-phospholipid interaction at high cholesterol regime (>45 mol %) was investigated. We aimed at understanding the cholesterol lateral distributions and cholesterol solubility limit in dioleoyl-phosphatidylcholine (DOPC or di18:1PC) bilayers.

Previously, we have measured the solubility limit of cholesterol in lipid membranes, χ^*_{chol}, using x-ray diffraction. Above this limit, cholesterol precipitates from the lipid bilayer to form cholesterol monohydrate crystals. We found that cholesterol solubility limits in the phosphatidylethanolamine (16:0,18:1-PE) and phosphatidylcholine (di12:0-PC, di16:0-PC, di22:1-PC, and 16:0,18:1-PC) were 50 and 67 mol%, respectively (Huang et al., 1999). The physical meaning of cholesterol solubility limit can be explained by our ''Umbrella model.'' According to this model, cholesterol is largely a hydrophobic molecule, and the small hydroxyl group cannot completely shield the rest of the hydrophobic body from water by itself. In a bilayer, cholesterol relies on polar phospholipid headgroup coverage to avoid the unfavorable free energy of exposing to water. This hydrophobic interaction provides a favorable attraction between cholesterol and phospholipid, or an unfavorable energy penalty for cholesterol cluster formation. When the concentration of cholesterol increases to the point at which large

Submitted July 8, 2003, and accepted for publication October 23, 2003.

Address reprint requests to Dr. Juyang Huang, Dept. of Physics, Texas Tech University, Lubbock, TX 79409. Tel: 806-742-4780; Fax: 806-742-1182; E-mail: juyang.huang@ttu.edu.

0006-3495/04/03/1532/13 $2.00

clusters of cholesterol form and not all cholesterols can be effectively covered by neighboring phospholipid headgroups, cholesterol begins to precipitate from the bilayer.

The cholesterol coverage requirement can be modeled as a form of multibody interaction. Monte Carlo simulations based on the Umbrella model showed a direct connection between cholesterol solubility limit and formation of regular distribution domains in a lipid bilayer. To satisfy the coverage requirement, cholesterol molecules distribute in a bilayer in such a way that the size of cholesterol clusters (or equivalently, the number of cholesterol-cholesterol contacts) is minimized. As cholesterol concentration increases in a bilayer, fewer and fewer numbers of lateral distributions can satisfy the coverage requirement. At the cholesterol solubility limit, a cholesterol-phospholipid bilayer can only adapt a few highly ordered lateral distributions to satisfy the coverage requirement (Huang and Feigenson, 1999). Our simulation showed that cholesterol precipitation and formation of regular distributions of lipids are most likely to occur near three discrete values of cholesterol mol fraction, 0.50, 0.57, and 0.67, which correspond to cholesterol/phospholipid mol ratios of 1/1, 4/3, and 2/1, respectively. Two interesting predictions came out of the simulations: i), at the cholesterol solubility limit, there is a highly ordered regular distribution of lipid in bilayers; and ii), in a PC bilayer with the cholesterol solubility limit of 0.67, if the unfavorable cholesterol-cholesterol interaction increases nonlinearly as the number of cholesterol contacts (described as Multibody Interaction Energy Parameter Set (MIEP) IV in Huang and Feigenson (1999)), there should be a cholesterol regular distribution (a hexagon pattern) at the cholesterol mol fraction of 0.50, a dimer pattern at 0.57, and a maze pattern at the solubility limit 0.67 (Huang and Feigenson, 1999). The regular distribution at $\chi_{chol} = 0.57$ had not been observed previously, and was only predicted from our simulation based on our Umbrella model.

Because these predictions are quite specific, an experimental investigation can provide a rigorous test to the model. In this study, regular distribution of cholesterol at high mol fraction of cholesterol and cholesterol solubility limit in DOPC bilayers were investigated by light scattering, optical microscope, fluorescence anisotropy, and fluorescent resonance energy transfer (FRET) techniques. Monte Carlo simulations were used to gain the understanding of the experimental data. We found that the anisotropy of diphenylhexatrience chain-labeled phosphatidylcholine (DPH-PC) in these liposomes exhibited local maxima at cholesterol mol fractions of 0.50 and 0.57, and a sharp drop at 0.67. The FRET efficiency from dehydroergosterol (DHE) to DPH-PC displayed a steep jump at cholesterol mol fraction of 0.5, and dips at 0.57 and 0.68. The result indicates the presence of highly ordered cholesterol regular distribution domains at these critical compositions. The solubility limit of cholesterol in DOPC bilayers, measured by light scattering and optical microscopy, was found to be 0.67 ± 0.02, which agrees favorably with our prediction that cholesterol form a regular distribution in a lipid bilayer at its solubility limit. The results strongly support the validity of the Umbrella model.

Cholesterol mol faction in most mammalian cell membranes is between 0.2 and 0.5. However, it has been reported that in fiber cells of lens of the eye, the mol fraction of cholesterol is as high as 0.67 (Li et al., 1985, 1987). The majority of cholesterol studies have been focused on lipid mixtures with cholesterol mol fraction <0.5, whereas investigations of cholesterol-lipid interaction at high cholesterol regime are relatively rare. A crucial feature of this study is sample preparation. Special cares must be taken to preparing liposomes with high cholesterol content. In our previous x-ray diffraction experiments, we found that demixing of cholesterol can occur during conventional sample preparation (dry film method or lyophilization method) and that this demixed cholesterol may produce artifactual cholesterol crystals (Huang et al., 1999; Buboltz and Feigenson, 1999). Therefore, phospholipid/cholesterol suspensions, which are prepared by conventional methods, may have falsely low cholesterol solubility limits and nonuniform liposome compositions. In this study, the Low Temperature Trapping (LTT) method, which was specifically designed to prevent demixing (Huang et al., 1999), was used to prepare DOPC/cholesterol mixtures.

MATERIAL AND METHODS

Materials

DOPC and POPC were purchased from Avanti Polar Lipids (Alabaster, AL) and cholesterol from Nu Chek Prep (Elysian, MN). Lipid purity (>99%) was confirmed by thin layer chromatography (TLC) on washed activated silica gel plates (Alltech Associates, Deerfield, IL) and developed with chloroform/methanol/water = 65:25:4 for phospholipid analysis or with petroleum ether/ethyl ether/chloroform = 7:3:3 for cholesterol analysis. The TLC plates were visualized by heating on a 200°C hotplate for 2 h after spraying with 20% ammonium sulfate solution. All solvents were of HPLC grade. Fluorescent lipid, 1-palmitoyl-2-((2-(4-(6-phenyl-*trans*-1,3,5-hexatrienyl)phenyl)ethyl)carbonyl)-3-*sn*-PC (DPH-PC), was obtained from Molecular Probes (Eugene, OR). DPH-PC consists of a 16-carbon saturated fatty acyl chain attached to the *sn*-1 position of the glycerol backbone and a diphenylhexatriene (DPH) fluorophore attached to the *sn*-2 position of the glycerol backbone via a short propanoyl chain. Dehydroergosterol was purchased from Sigma Chemical (St. Louis, MO). Concentrations of phospholipid stock solutions were determined by a phosphate assay (Kingsley and Feigenson, 1979). Aqueous buffer (pH 7.0, 5 mM PIPES, 200 mM KCl, 1 mM EDTA, 1 mM NaN_3) was prepared from deionized water ($\sim$18 MΩ) and filtered through a 0.1-μm filter before use.

DOPC/cholesterol liposome preparation

Compositionally uniform DOPC/cholesterol liposomes were prepared using the LTT method, which was specifically designed to prevent lipid demixing (Huang et al., 1999). Briefly, DOPC and cholesterol were dissolved and mixed in chloroform. For FRET measurement, premixed DHE, and DPH-PC in chloroform at 10:1 ratio was added to the mixtures. For anisotropy measurement, only DPH-PC was added. The total amount of lipid in each

sample was fixed at 0.2 μmol or 2 μmol for fluorescence or microscopy measurements, respectively. Chloroform was first removed under a vacuum of 30 mTorr for 12 h. The dry lipid films were redissolved in dry chloroform containing 2% of methanol. These mixtures were then frozen in liquid nitrogen and subsequently lyophilized at a controlled temperature (from -20 to -70°C) in such a way that the chloroform in the mixtures remained solid. After the bulk solvent had been removed, the lipid powder was kept at -20°C under a vacuum of 30 mTorr for another 12 h or more to remove any residual solvent. Just before hydration, the samples were warmed to room temperature in a stirring water bath for 1 min. Two milliliters of aqueous buffer was added to the dry lipid powder immediately followed by 5 min vortexing. To increase sample concentration for microscopy study, only 1/2 ml of buffer was added. The samples were prepared and sealed under argon under dim red light. The liposomes were stored at 23°C in the dark on a mechanical shaker for ~10 days before the fluorescence measurements. The samples were vortexed vigorously once a day during the equilibration period. TLC measurements revealed no degradation of the bulk lipids during the equilibration.

Optical microscopy

Optical microscopy was used to detect the presence of cholesterol crystals in the lipid dispersions. The method has been described previously (Huang et al., 1999). An Olympus (Melville, NY) IX70 inverted microscope was used in the Nomarski differential interference contrast (Nomarski DIC) mode. An Olympus 20× air (UplanFl) or 60× water immersion (UplanApo) objective was used. Images were captured by a Cooke SensiCam digital CCD camera (Auburn Hills, MI). Hydrated DOPC/cholesterol dispersions (at 4 mM) made by the LTT method were viewed on thin coverglasses. The advantage of light microscopy is that cholesterol monohydrate crystals and lipid vesicles can be identified by direct, visual observation (Loomis et al., 1979). We examined a series of samples with varying compositions and searched for the critical composition above which the presence of crystals of cholesterol monodydrate was detected. The main limitation of the method is that the quantity of crystals cannot be estimated, due to the small sampling volume and variations in the crystal size. However, light microscopy can serve as a supporting technique to confirm χ^*_{chol} value.

Fluorescence anisotropy and FRET

Steady-state anisotropy r of DPH-PC and fluorescence resonance energy transfer efficiency between DHE and DPH-PC were measured with a T-mode Photon Technology International (Lawrenceville, NJ) C61/2000 spectrofluorimeter. In FRET experiments, the DPH-PC:DHE:lipid ratio was fixed at 1:10:1000. In anisotropy experiment, the DPH-PC:lipid ratio was 1:1000. The excitation monochromator was set at 310 nm with 4-nm slit width, and emission fluorescence intensities were collected at 371 nm (DHE emission peak) and 430 nm (DPH-PC emission peak) with 6-nm slit width. The fluorescence intensity ratio, I_{430}/I_{371}, was used as a measure of the energy transfer efficiency. Use of the intensity ratio largely eliminated the noise introduced by variations in lipid and probe concentration between samples. Steady-state anisotropy r of DPH-PC was calculated as $(I_{||} - gI_{\perp})/(I_{||}+2gI_{\perp})$, where $I_{||}$ and $I_{\perp}$ are emission intensities at 430 nm from the parallel and perpendicular polarization and g is the g-factor related with relative sensitivity of the two emission channels and can be obtained with the excitation polarization is set to perpendicular (Gratton et al., 1984). The detectors were set in the photon counting mode and the average intensities were obtained from a 40-s time scan.

Light scattering

Ninety-degree light scattering was measured using the same PTI spectrofluorimeter. The incident beam was set at 550 nm with a 2-nm slit width. To avoid detector saturation, the 90° scattering light was collected with the detection monochromators set at 4 nm higher than the incident wavelength. The diameter of the illumination beam in the cuvette was narrowed down to ~2 mm by adjusting the focus lens. Two milliliters of 100 μM DOPC/cholesterol suspension was added to the cuvette with a Teflon coated magnetic stir bar. Determination of χ^*_{chol} by light scattering exploits the differences in size, structure, and refractive index between cholesterol crystals and bilayer vesicles. As cholesterol crystals enter or leave the narrow illumination beam due to stirring motion, fluctuations were introduced in the scattering intensity. To reduce the background scattering fluctuation by large multilamellar vesicles, the samples were sonicated in a low-power NEY sonication bath (Ultrasonik 3000, Yucaipa, CA) for 10 s, then vortexed vigorously for 5 min per day during the incubation period. The scattering signals from both detector channels were collected in the photon counting mode at a rate of 10 data points/s for a total of 60 s.

Monte Carlo computer simulation

Lateral distributions of lipids with $\chi_c > 0.45$ were generated by Monte Carlo simulation to help understand the experimental data. The microscopic molecular interaction model and computer simulation method have been described in detail previously (Huang and Feigenson, 1999). In earlier studies, we found that the dominated lipid interaction in a lipid bilayer containing high cholesterol content is an unfavorable cholesterol-cholesterol multibody interaction. This interaction increases nonlinearly as the number of cholesterol-cholesterol contacts. This nonlinear increase is the key of producing a series of regular distributions of cholesterol at some well-defined lipid compositions, i.e., at $\chi_c = 0.5$, 0.57, and 0.67. In this study, we used a very simple form of cholesterol multibody interaction: the energy cost for each additional cholesterol-cholesterol contact was chosen to be one unit higher than the preceding one, which was named as the Multibody Interaction Energy Parameter Set IV in Huang and Feigenson (1999). We have shown that with this interaction parameter set, the chemical potential of cholesterol jumped at $\chi_c = 0.5$, 0.57, and 0.67, a definitive indication that a large-scale regular distribution was produced at these compositions (Huang and Feigenson, 1999).

Simulating superlattices encounters a unique simulation size requirement: each regular distribution pattern has its own periodicity. A perfect regular distribution pattern can only be generated if the size of the simulation lattice is multiple of the pattern periodicity. Otherwise, defects will be introduced. The periodicities for regular distributions at cholesterol mol fraction 0.50, 0.57, and 0.67 are 6, 10, and 8, respectively. The simulation lattice used in this study is 120×120, and can accommodate all three regular distributions.

Simulations were performed on a triangular lattice with the standard periodical boundary condition. Based on our previous studies, the size effect is negligible (Huang and Feigenson, 1993; Huang, 2002). Neighboring cholesterols and acyl chains can exchange their position with a probability given by the Metropolis method (Metropolis et al., 1953). All simulations started from an ideal mixture of a given composition. The typical equilibrium time was 20,000–60,000 Monte Carlo steps. Statistical values were obtained through a 10,000 Monte Carlo steps average after equilibrium. At superlattice compositions, multiple superlattice domains (with different orientations) usually form at the beginning. Eventually, one domain would take over all the others and cover the entire simulation lattice. From that point on, the superlattices become quite stable with very few defects.

RESULTS

The maximum solubility of cholesterol (χ^*_{chol}) in DOPC bilayers has not been measured previously. We have shown that equilibrium and reproducible χ^*_{chol} can be obtained if samples were prepared by the Low Temperature Trapping method or by the Rapid Solvent Exchanging method (Huang et al., 1999; Bubultz and Feigenson, 1999). In this study, all

samples were prepared by the LTT method. Ninety-degree light scattering and optical microscopy were used to determine the χ^*_{chol} in DOPC bilayers.

Light scattering can detect the presence of cholesterol crystals in samples because of the difference in scattering property between multilamellar vesicles and cholesterol crystals. As cholesterol crystals enter or leave the illumination beam (~2 mm in diameter) in a cuvette due to stirring motion, large fluctuations are introduced in the scattering intensity. Fig. 1 shows the light scattering intensities as a function of time for two DOPC/cholesterol mixtures near χ^*_{chol}. The sample with $\chi_{chol} = 0.64$ was below the χ^*_{chol} in DOPC, therefore contained no cholesterol crystals; whereas the sample with $\chi_{chol} = 0.74$ was above the χ^*_{chol}, thus contained some cholesterol crystals. The fluctuation in scattering intensity was much larger in the sample of $\chi_{chol} = 0.74$ than in the sample of $\chi_{chol} = 0.64$. We used the standard deviation σ normalized by the average intensity I as a parameter to measure the fluctuation, which corrected the concentration variation between samples. Fig. 2 shows σ/I as a function of cholesterol mol fraction. The fluctuation parameter σ/I rapidly increased around $\chi_{chol} = 0.67$, which indicates that cholesterol crystals begin to form at this composition. The measured χ^*_{chol} value from five independent experiments was 0.67 ± 0.02.

To test whether the brief low-power sonication changes the solubility limit of cholesterol in a bilayer, we performed a control experiment with 16:0,18:1PC (POPC). The χ^*_{chol} value in POPC was previously found to be 0.67 determined by x-ray diffraction (Huang et al., 1999). The χ^*_{chol} value measured by our light scattering was also 0.67 (data not shown), very similar to Fig. 2. This suggests that light scattering is a valid method to detect χ^*_{chol} in PC bilayers.

We also searched the value of χ^*_{chol} using optical microscopy. Fig. 3 *a* is a Nomarski DIC image of a DOPC/cholesterol sample with $\chi_{chol} = 0.63$, in which no cholesterol crystal was detected. Fig. 3 *b* is a DIC image for a sample

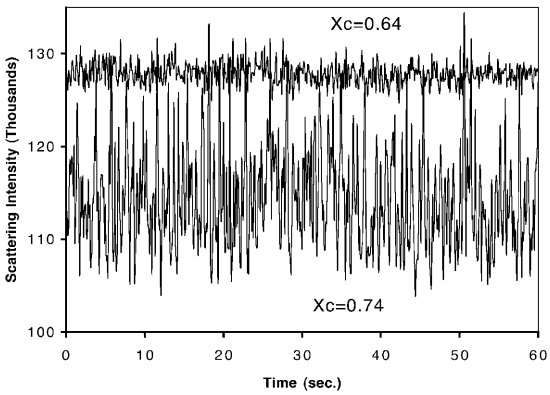

FIGURE 1 Ninety-degree light scattering intensities as a function of time. (*Top trace*) Intensity fluctuation from a DOPC/cholesterol mixture with $\chi_c = 0.64$. (*Bottom trace*) From a DOPC/cholesterol mixture with $\chi_c = 0.74$.

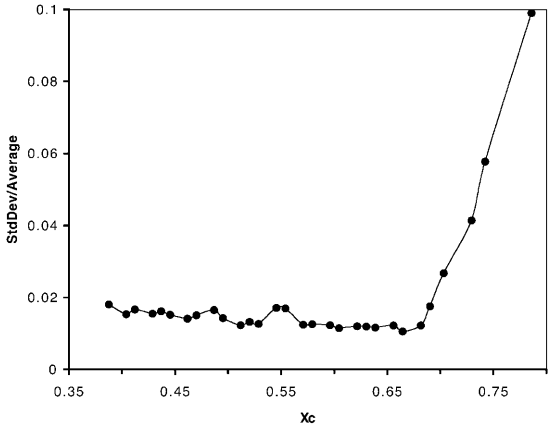

FIGURE 2 Standard deviation of light scattering intensity normalized by the average intensity as a function cholesterol mol fraction in DPPC/cholesterol mixtures. The sharp rise near $\chi_c = 0.68$ is caused by scattering of cholesterol monohydrate crystals.

with $\chi_{chol} = 0.69$, in which a number of cholesterol crystals are visible. After examining three independent sample series, the value of χ^*_{chol} in DOPC bilayers was determined to be 0.66 ± 0.02, which was consistent with the light scattering result.

Fig. 4 *a* shows four sets of independent measurement of FRET efficiency between DHE and DPH-PC (I_{430}/I_{371}) as a function of cholesterol mol fraction. To facilitate viewing and comparing, curves were vertically displaced. Even though no two curves look exactly the same, a general pattern emerges: each curve shows a sharp jump around $\chi_{chol} \approx 0.5$, and dips around $\chi_{chol} \approx 0.57$ and 0.67. The three vertical shaded bars on the figure indicate the compositions of predicted regular distribution at $\chi_{chol} = 0.50, 0.57$, and 0.67, and the width of the bars reflects the experimental uncertainty

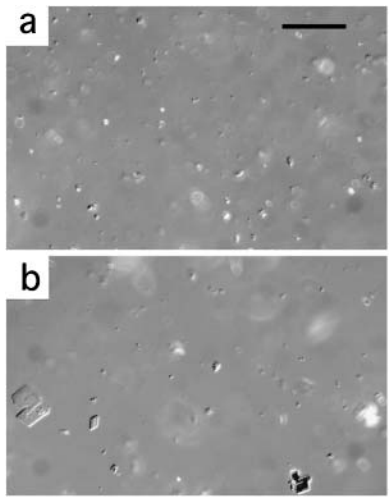

FIGURE 3 DIC microscope images of DOPC/cholesterol mixtures. (*Top*) A sample with $\chi_c = 0.63$; no cholesterol crystal was found. (*Bottom*) A sample with $\chi_c = 0.69$, some cholesterol crystals were visible. (*Black bar*) 10 μm.

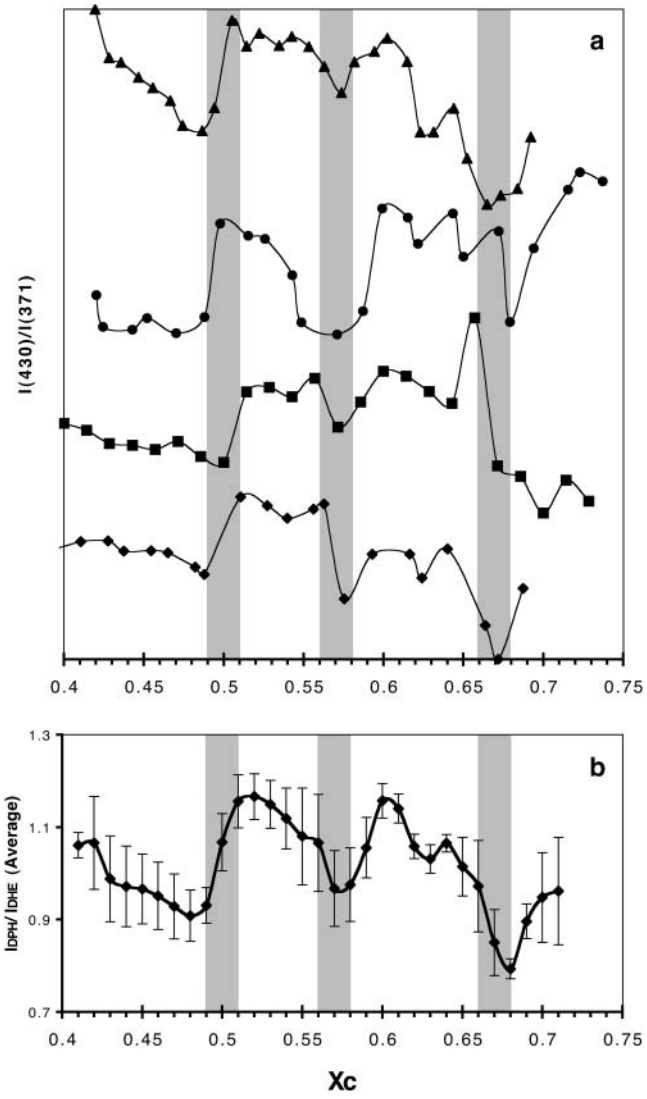

FIGURE 4 Fluorescence resonance energy transfer parameter between DHE and DPH-PC, $I(430)/I(371)$, as a function of cholesterol mol fraction in DOPC/cholesterol mixtures. (*a*) Raw data from four independent sample sets. Curves were vertically displaced to facilitate viewing. (*b*) The average curve of the four measurements.

in absolute value of lipid composition (± 0.01) for our samples. As shown in Fig. 4 *a*, the locations of jump and dips agree quite well with the predicted regular distribution compositions.

The jumps of FRET efficiency at $\chi_{chol} \approx 0.50$ were quite sharp. Fig. 5 shows the fluorescence emission spectrum of two consecutive samples around $\chi_{chol} = 0.50$. The emission spectrums of DHE and DPH-PC in 1/1 DOPC/cholesterol vesicles are shown in the lower portion of the figure, and their maximum peaks are at 371 nm and 430 nm, respectively. The intensity ratio I_{430}/I_{371} change abruptly within 1 mol% change of cholesterol mol fraction.

The average of the four curves in Fig. 4 *a* is shown in Fig. 4 *b*. Because the lipid compositions of data points in each experiment were different, the average was carried out in the following way: first, the adjacent points in each curve were simply connected by straight lines without smoothing; then a simple average was performed on these four lines from $\chi_{chol} = 0.41$ to 0.72 at 0.01 interval to obtain the average curve. The height of the error bars indicates the standard deviations. The average curve shows a jump at $\chi_{chol} \approx 0.5$, and dips at 0.57 and 0.68. It should be pointed out that the estimated experimental uncertainty in absolute value of lipid composition for our samples was $\pm 1\%$, whereas the relative uncertainty in the same data set was 0.2%. Therefore, in Fig. 4 *a*, the sharpness of the jump or dip is more reliable than their absolute positions. The average curve in Fig. 4 *b* is less noisy, but the sharpness of the jump around 0.50 got smoothed out considerably.

Fig. 6 *a* shows three sets of independent measurement of steady-state fluorescence anisotropy r of DPH-PC as a function of χ_{chol}. The average of the three measurements is shown in Fig. 6 *b*, which was obtained the same way as Fig. 4 *b*. In Fig. 6 *b*, r has a small local maximum at $\chi_{chol} = 0.50$, a prominent peak at 0.57, and a sharp drop at 0.67.

There is a small dip at $\chi_{chol} \approx 0.63$ in the average curve of FRET efficiency (Fig. 4 *b*) as well as in anisotropy of DPH (Fig. 6 *b*). The dips are shallower than others and are not obvious by inspecting original data curves (Figs. 4 *a* and 6 *a*). However, it may be real because they occur at the same composition in two different measurements. More study is certainly needed to confirm this dip.

Monte Carlo simulation was used to visualize the lateral distribution of lipids. Fig. 7 shows snapshots of computer-simulated lateral distribution of lipid at the regular distribution compositions and in between. The distributions are shown in 40×40 size, although the simulations were carried on 120×120 lattices. The cholesterol multibody interaction energy parameter ΔE_c was fixed at 2 kT, high enough to generate all three regular distributions. The lateral distribution at 0.50 (Fig. 7 *b*) is a ''hexagonal pattern'' regular distribution, at 0.57 (Fig. 7 *d*) is a ''dimer pattern'' regular distribution, and at 0.67 (Fig. 7 *f*) is a ''maze pattern'' regular distribution. These regular distributions have a very long-range order: a single pattern covers the entire 120×120 simulation lattice. Fig. 7 *c* is a lateral distribution at $\chi_c = 0.53$, and it contains many small domains of both ''hexagonal pattern'' and ''dimer pattern.'' Fig. 7 *e* is a lateral distribution at $\chi_{chol} = 0.60$, in which small domains of ''dimer pattern'' and ''maze pattern'' and defect regions coexist. In a computer-simulation study, Sugar et al. (1994) suggested that the size of regular distribution domains become maximum at critical cholesterol mol fractions, and regular distribution domains and irregular distributions coexist at compositions between the critical mol fractions. The lipid lateral distributions in Fig. 7 are consistent with their finding.

We also investigated the extent of regular distribution as a function of the magnitude of interaction energy. The

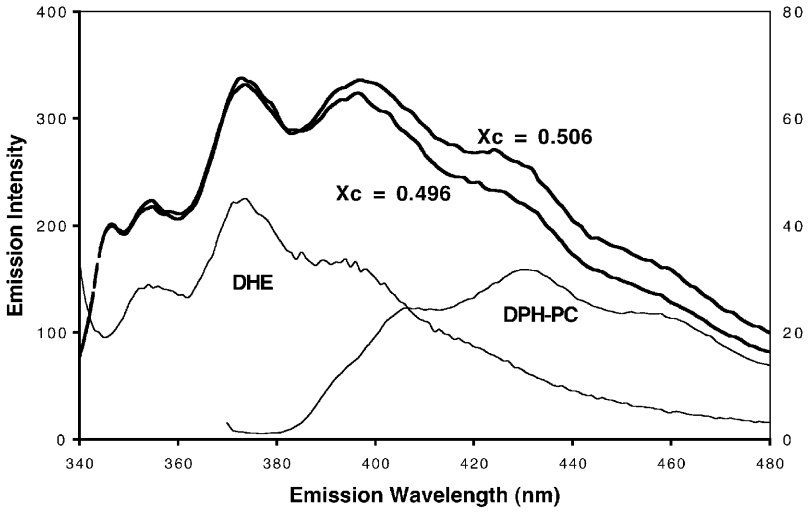

FIGURE 5 Sharp jump of FRET efficiency near $\chi_c = 0.5$. (*Lower right*) Fluorescence emission spectrum of DPH-PC in 1/1 DOPC/cholesterol vesicles. (*Lower left*) Fluorescence emission spectrum of DHE in 1/1 DOPC/cholesterol vesicles. (*Upper*) Fluorescence emission spectrums of DOPC/cholesterol mixtures of $\chi_c = 0.496$ and 0.506, labeled with both DHE (1%) and DPH-PC (0.1%).

cholesterol regular distributions at $\chi_{chol} = 0.50$ (Fig. 7 *b*), 0.57 (Fig. 7 *d*), and 0.67 (Fig. 7 *f*) can be characterized by each cholesterol having exactly zero, one, and two cholesterol-cholesterol contacts. Let $N_c(0)$, $N_c(1)$, and $N_c(2)$ be the number of cholesterol having exactly zero, one, and two cholesterol-cholesterol contacts, respectively, and N_c be the total number of cholesterol molecules. We can define $N_c(0)/N_c$ as an order parameter to describe the fraction of cholesterol molecules in the 0-cholesterol contact state. The order parameter becomes 1, if a perfect hexagonal regular distribution pattern covers the entire lateral surface at $\chi_{chol} = 0.50$. Similarly, we can define $N_c(1)/N_c$ and $N_c(2)/N_c$ as order parameters for the dimer and maze patterns, respectively. Fig. 8 shows three order parameters as a function of the magnitude of multibody interaction energy parameter ΔE_c. Let's use the dimer pattern as an example (*middle panel* in Fig. 8). Fig. 9 shows snapshots of lipid lateral distribution at $\chi_{chol} = 0.57$ with various values of ΔE_c. When $\Delta E_c = 0$, the mixing of cholesterol and DOPC is ideal (i.e., random). The order parameter $N_c(1)/N_c$ is ~0.19. A snapshot of the random lateral distribution is shown in Fig. 9 *a*. As ΔE_c increases, the order parameter $N_c(1)/N_c$ increases, i.e., more and more cholesterol adapt the 1-contact state (Fig. 9, *b–d*). However, the size of aligned dimer domains is small and there is no long-range order of cholesterol distribution. Around $\Delta E_c = 1.8$ kT, the magnitude of interaction energy reaches the critical value, the order parameter $N_c(1)/N_c$ jumps steeply to its maximum value of 1, which indicates that all cholesterol molecules are in the dimer state. A single stable aligned dimer domain covers the entire lateral surface and a long-range order of the molecules has been established (Fig. 9 *e*).

There are some important differences in lipid lateral distribution before and after the interaction energy reaches the critical value. When the interaction energy is lower than the critical value, regular distribution domains are small and lack long-range order. More importantly, they are dynamic domains, i.e., they form and fade away continuously. On the other hand, when the interaction energy reaches the critical value, once a large long-range ordered regular distribution pattern covers the entire simulation lattice, the distribution becomes very stable: it stays virtually unchanged.

As illustrated in Figs. 8 and 9, a perfect dimer pattern with long-range order of cholesterol does not form until ΔE_c reaches ~1.8 kT. However, small dynamic domains of the dimer pattern can form at much lower value of interaction energy. For example, at as low as 0.5 kT, statistically, >40% of cholesterol already in the dynamic dimer pattern domains. Similar conclusions can be drawn for regular distributions at 0.50 and 0.67.

In our simulations, two acyl chains belonging to the same phospholipid are not physically linked. This can result in some unrealistic configurations in which single hydrocarbon chain is surrounded with cholesterol molecules (Fig. 9 *a*). However, this problem essentially vanishes as the magnitude of multibody interaction energy increases (Fig. 9, *b–e*). Thus, it should not significantly affect our main conclusion. Sugar et al. (1998) have used a simulation procedure to link two acyl chains. We will try to incorporate it in our future simulations.

In Fig. 8, the order parameter $N_c(2)/N_c$ at $\chi_{chol} = 0.67$ (*bottom panel*) does not have as steep a jump as the other two order parameters. This is because the maze pattern is actually a mixture of two regular distribution patterns (Huang and Feigenson, 1999). Substantial interfacial regions suppress the order parameter and the sharpness of the transition.

DISCUSSION

Maximum solubility of cholesterol in DOPC

In this study, the maximum solubility limit of cholesterol in DOPC bilayers determined by the combination of light scattering and optical microscopy methods was found to be 0.67 ± 0.02. This is similar to the χ^*_{chol} values in the other four phosphatidylcholine bilayers (di12:0-PC, di16:0-PC,

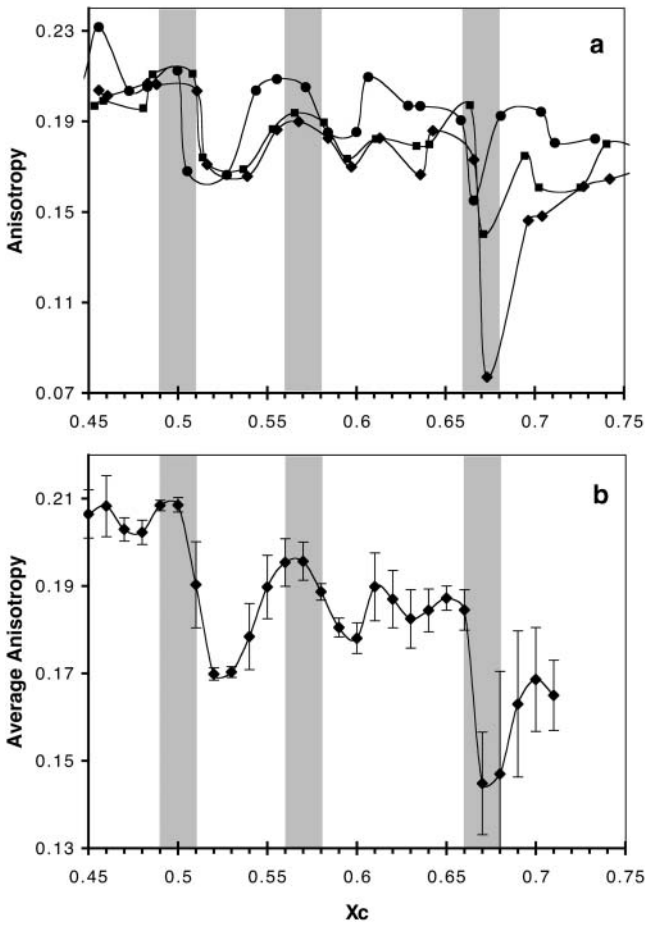

FIGURE 6 Steady-state fluorescence anisotropy of DPH-PC as a function of cholesterol mol fraction in DOPC/cholesterol mixtures. (*a*) Raw data from three independent samples sets. (*b*) The average curve of the three measurements.

di22:1-PC, and 16:0,18:1-PC) previously measured by synchrotron x-ray diffraction. This result is consistent with the prediction of the Umbrella model in which the value of χ^*_{chol} reflects the ability of PC to cover the neighboring cholesterol clusters. The coverage is determined by the effective size of phospholipid headgroups and the cross-sectional area of PC acyl chains at the position where the cholesterol resides in the lipid bilayer. For the saturated phospholipids with the same headgroup, such as PC, the difference in the PC's chain length may not change the cross-sectional area of the acyl chain to a significant extent. Thus, similar values of χ^*_{chol} for the above four PC bilayers are expected. However, DOPC does differ from those PCs by having two double bonds in the C9 position of its oleoyl chains. If the presence of both double bonds interferes with the cholesterol packing, we would have expected a lower χ^*_{chol} value. Yet, our result suggests that the double bonds at the C9 position have very little effect on the packing of cholesterol in the DOPC bilayer.

Cholesterol interaction with lipids of different acyl chains has been a topic of great interest. It has been shown that cholesterol has low affinity to unsaturated acyl chains and can selectively form association with saturated chains in a mixed chain environment (Mitchell and Litman, 1998; Niu and Litman, 2002). Our observation that the double bonds have little effect on χ^*_{chol} value is not totally surprising. Recently, Wang et al. (2002) measured the formation of cholesterol superlattices at low cholesterol concentration using fluorescence measurements. They found that cholesterol superlattice becomes undetectable when the *cis* double bond of PC is located at the same level of cholesterol steroid ring, i.e., between C8 and the carboxyl carbon. Because the double bond on an oleoyl chain is at the C9 position, it should not affect the packing of cholesterol in DOPC bilayer. However, if a double bond is located at a higher position, such as in di18:1c6-PC, it may result in a lower χ^*_{chol} value.

FRET between DHE and DPH-PC

This is the first study using FRET technique to investigate regular distributions of lipid in a bilayer. Previously works usually involved one fluorescence probe. In this study, dehydroergosterol, a natural cholesterol fluorescent analog, was used as the donor molecule and diphenylhexatriene chain-labeled phosphatidylcholine was used as the receptor molecule. In a FRET experiment, the rate of transfer of energy from a donor to an acceptor strongly depends on the distance between the donor and acceptor, i.e., to the inverse sixth power of the distance (Förster, 1948). In addition, the rate also depends on the relative orientation of the transition dipole moments of the donor and acceptor (Dale et al., 1979; Lakowicz, 1983). In Fig. 4, FRET efficiency shows a sharp jump around $\chi_c = 0.5$, a dip at 0.57, and a drop at 0.67. All three compositions have been previously predicted to be the regular distribution compositions (Huang and Feigenson, 1999). The FRET data indicate an abrupt change in the distance and/or the relative dipole orientation between the donor (DHE) and the acceptor (DPH-PC) at these three critical compositions.

DHE differs from cholesterol only in having three additional double bonds and an extra methyl group. It has been found that DHE behaves quite like cholesterol in lipid bilayers (Schroeder et al., 1991; Mukherjee et al., 1998). Liu et al. (1997) found that DHE and cholesterol are interexchangeable in forming cholesterol regular distributions. It is reasonable to assume that DHE molecules will occupy the sites that would otherwise be occupied by cholesterol in case of regular distribution. On the other hand, because of the bulking fluorescence group on the acyl chain of DPH-PC, it has less room in the acyl chain region to accommodate cholesterol. Using the argument of the Umbrella model, DOPC can provide better coverage for cholesterol than DPH-PC, so DPH-PC should have less affinity to cholesterol than DOPC.

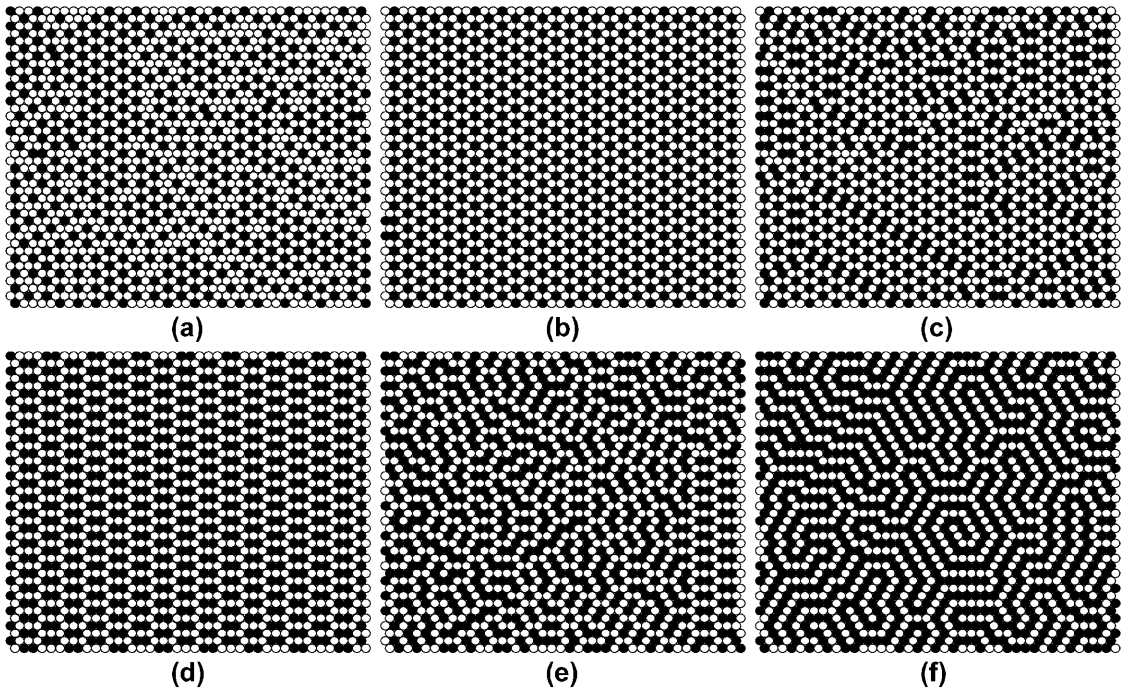

FIGURE 7 Snapshots of cholesterol-DOPC lateral distributions at some critical regular distribution compositions and compositions between regular distributions, simulated with the Multibody Interaction Energy Parameter Set IV in Huang and Feigenson (1999). The cholesterol multibody interaction energy parameter ΔE_c was fixed at 2 kT. (*a*) $\chi_c = 0.44$; (*b*) $\chi_c = 0.50$, a ''hexagonal pattern'' regular distribution; (*c*) $\chi_c = 0.53$; (*d*) $\chi_c = 0.57$, a ''dimer pattern'' regular distribution; (*e*) $\chi_c = 0.60$; and (*f*) $\chi_c = 0.67$, a ''maze pattern'' regular distribution. (○) Acyl chain; (●) cholesterol.

When the cholesterol mol fraction is below 0.5, there will be some lattice sites having no cholesterol contact (see Fig. 7 *a*). Because DPH-PC has a low affinity to cholesterol, it will preferentially occupy these sites, away from cholesterol (or DHE). Thus, the FRET efficiency will be lower. However, if a cholesterol regular distribution formed at $\chi_{chol} = 0.5$, then all the acyl chain sites should have three nearest-neighbor contacts with cholesterol (see Fig. 7 *b*). DPH-PC would have no choice, but to occupy these sites with close contacts with cholesterol (or DHE). Thus, the average distance between DPH-PC and DHE is shortened suddenly at $\chi_c = 0.5$, and gives rise to a sharp jump of FRET efficiency.

The dips in FRT efficiency at $\chi_c = 0.57$ and 0.67 are likely resulted from the change in the relative dipole orientation of DHE and DPH-PC due to regular distributions (Dale et al., 1979; Lakowicz, 1983). When χ_{chol} is higher than 0.5, the density of cholesterol is so high that all acyl chain sites have close contacts with cholesterol (or DHE), independent of the lipid lateral distribution (see Fig. 7). Thus, the average distance between DHE and DPH-PC does not change much. Regular distributions are highly ordered lateral packing structures. It is reasonable to assume that the orientation free volume of the electric dipole of DPH-PC or DHE is more restricted within a regular distribution domain. It is likely that FRET efficiency can be reduced if the relative orientation of DHE dipole and DPH-PC dipole has a smaller probability to reach the favorable angle for optimum FRET within the lifetime of the DHE excited state.

With the excitation wavelength of 310 nm, a certain population of DPH-PC emission is due to the direct excitation of the DPH fluorophore. We are aware that changes in fluorescence intensity of DHE or DPH-PC, independent of the FRET process, can also alter the I_{430}/I_{371} ratio. Previously, Chong's group studied the regular distributions of cholesterol in di14:0PC and di16:0PC bilayers using DHE as a probe (Chong, 1994; Liu et al., 1997). They found that the normalized fluorescence intensity and the average lifetime of DHE have dips at the predicted cholesterol regular distribution compositions. These two factors alone would cause peaks rather than dips to the I_{430}/I_{371} ratio. There is no direct information about the behavior of DPH-PC fluorescence intensity responding to a cholesterol regular distribution. A recent work on DPH-PC in POPC/cholesterol bilayers revealed only a modest drop in fluorescence lifetime corresponding to a cholesterol regular distribution (Cannon et al., 2003).

It is interesting that when the composition of cholesterol in a sample is higher than the solubility limit of cholesterol in DOPC (>0.67), FRET and anisotropy of DPH-PC both show an increase from the minima at 0.67 (Figs. 4 and 6). This suggests that the lipid packing in the bilayers becomes less ordered than that at $\chi_{chol} = 0.67$. Because the cholesterol

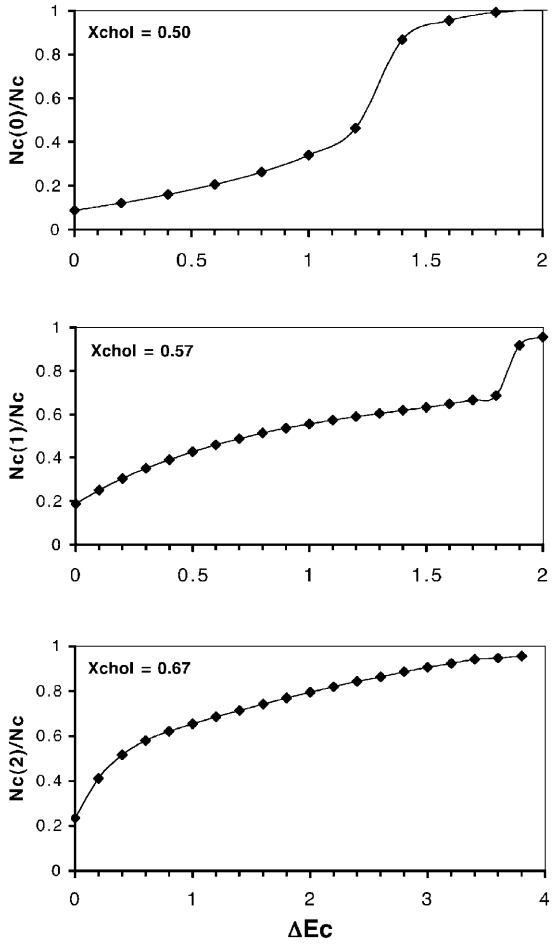

FIGURE 8 The fraction of total cholesterol in the corresponding regular distribution state as a function of the cholesterol multibody interaction energy parameter ΔE_c, at three regular distribution compositions. (*Top*) $\chi_c = 0.50$; (*middle*) $\chi_c = 0.57$; (*bottom*) $\chi_c = 0.67$.

solubility limit has been reached, the cholesterol concentration inside the bilayers should remain constant. The packing disorder is likely due to cholesterol microcrystal formation between lamellas. In previous x-ray diffraction experiments, it has been found that as soon as the cholesterol mol fraction passed the solubility limit and cholesterol monohydrate crystals began to form, the broad wide-angle diffraction peaks at 4.9 Å, corresponding to the acyl chain packing in the bilayers, quickly disappeared (Huang et al., 1999). This phenomenon was consistent in all the PC and PE mixtures we have studied.

Fluorescence anisotropy of DPH-PC

Steady-state fluorescence anisotropy of DPH-PC has a small local maximum at 0.50, a prominent peak at 0.57, and a sharp drop at 0.67 (Fig. 6 *b*). The maxima at 0.50 and 0.57 can be attributed to the fact that the membrane surface area covered by the highly ordered regular distribution domains reaches maximum at the critical mol fractions (Sugar et al., 1994). Thus, the anisotropy value of DPH-PC reflects the orientational order of the acyl chains in the DOPC/cholesterol bilayers. On the other hand, the sharp drop at 0.67 is likely due to a decrease in the orientational order of the acyl chains caused by the cholesterol microcrystal formation between the lamellas.

Regular distribution at $\chi_c = 0.57$ and driving force of regular distributions

The driving force of lipid regular distribution has long been interested by many researchers (see reviews in Somerharju et al. (1999) and Chong and Sugar (2002)). The original superlattice model emphasizes the difference in the cross-sectional area between the steroid ring and the neighboring phospholipid acyl chains. This difference would cause an elastic deformation in the hexagonal lipid lattices, thus providing a repulsion between the bulky steroid rings for achieving a maximum separation (Virtanen et al., 1988; Chong, 1994). Another hypothesis (Spacer model) focuses on the imbalance between the lipid headgroup and the acyl chain cross-sectional areas (Somerharju et al., 1999). The surface area occupied the strongly hydrated phosphocholine headgroup is larger than the cross-sectional area of the acyl chains. This imbalance leads both to the crowding of the headgroup level and looser packing of the acyl chains. However, when adequate amounts of a lipid with a relatively small headgroup (e.g., cholesterol, diglyceride, or PE) is mixed with PC, the crowding is diminished or abolished and the packing (order) of the acyl chains increases. The Superlattice model and Spacer model predict the maximum separation of ''spacer'' or ''foreign'' molecules and predict regular distributions by an equation based on pattern symmetry (Virtanen et al., 1988; Chong, 1994; Tang and Chong, 1992).

Recently, Huang and Feigenson (1999) proposed the Umbrella model to particularly describe the interaction between cholesterol and phospholipid molecules. It emphasizes that the polar phospholipid headgroups must help to cover the nonpolar body of cholesterol to avoid the unfavorable free energy of exposing the cholesterol to water. The interaction described by the Umbrella model can be expressed as a strong cholesterol-phospholipid multibody interaction in a computer simulation. This allows the quantitative analysis of the energy requirement for a simulated regular distribution. Monte Carlo simulations based on the Umbrella model have successfully generated regular distributions at 0.157, 0.25, 0.4, 0.5, 0.57, and 0.67 (Huang and Feigenson, 1999; Huang, 2002). In general, at high cholesterol concentrations, cholesterol distribute in a lipid bilayer in such way that the cholesterol cluster size is minimized; at low cholesterol concentration ($\chi_{chol} < 0.50$), the acyl chains of PC minimize the higher-order contacts with cholesterol to reduce the overall entropy penalty of chain ordering (Huang, 2002).

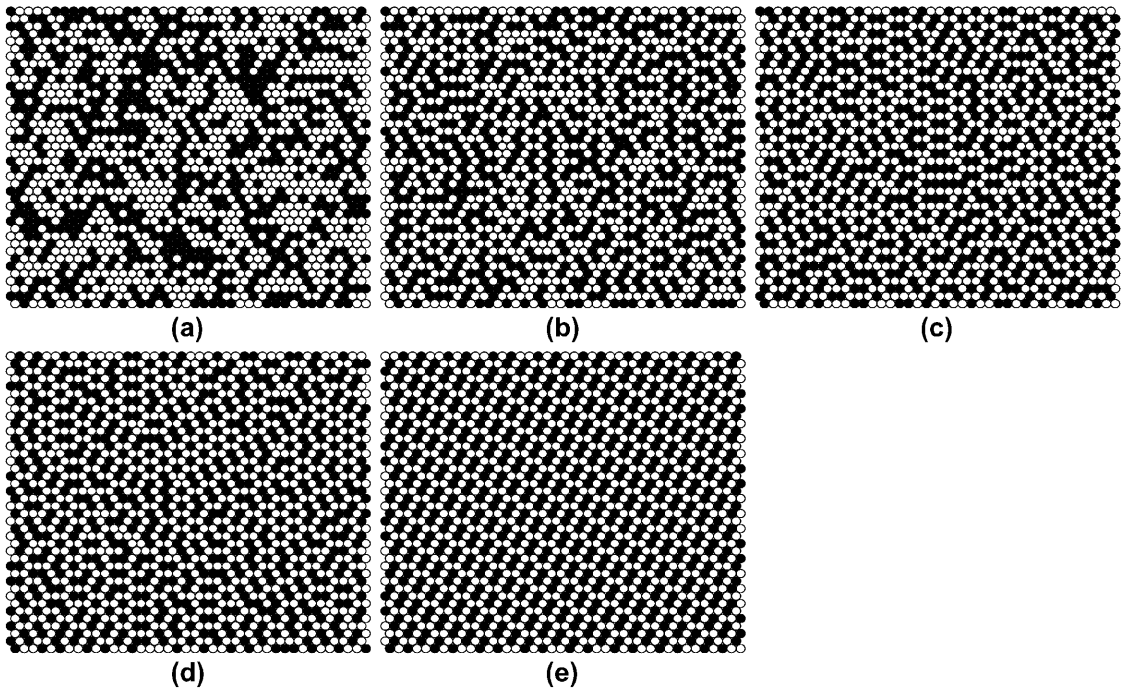

FIGURE 9 Snapshots of cholesterol-DOPC lateral distributions at $\chi_c = 0.57$ with various value of ΔE_c, simulated with the Multibody Interaction Energy Parameter Set IV in Huang and Feigenson (1999). (*a*) $\Delta E_c = 0$, a random distribution; (*b*) $\Delta E_c = 0.5\,kT$; (*c*) $\Delta E_c = 1.0\,kT$; (*d*) $\Delta E_c = 1.5\,kT$; and (*e*) $\Delta E_c = 2.0\,kT$, a long-range ordered dimer pattern. (○) Acyl chain; (●) cholesterol.

Regular distributions of cholesterol at the high cholesterol regime have some unique properties: i), the regular distributions, such as the dimer and the maze patterns, are neither hexagonal nor centered rectangular. Thus ''regular distribution'' is a more precise term than ''superlattice'' to describe the distribution behavior of cholesterol; ii), if it is assumed that each cholesterol molecule occupies one hexagonal lattice site, then the highest possible cholesterol mol fraction for regular distribution in the Superlattice or Spacer model is 0.50 (Virtanen et al., 1988; Chong, 1994; Tang and Chong, 1992). Chong and co-workers suggested that a cholesterol molecule may occupy two lattice sites at high cholesterol concentration and a modified equation can be used to predict the cholesterol regular distributions for $\chi_{chol} > 0.50$ (Chong, 1994; Tang and Chong, 1992). In the Umbrella model, a cholesterol molecule is assumed to occupy one lattice site. The dimer pattern (at 0.57) and the maze pattern (at 0.67) came out from a Monte Carlo simulation naturally by assuming that the unfavorable cholesterol-cholesterol multibody interaction increases nonlinearly with the number of cholesterol contacts (Huang and Feigenson, 1999). Note that the regular distribution at 0.57 has not been observed previously or predicted elsewhere. The experimental verification of the prediction at $X_c = 0.57$ in this study indicates that the Umbrella model captures the key molecular interactions between cholesterol and phospholipids.

Dynamic domains and magnitude of interaction

Sugar et al. (1994) made the first attempt to simulate regular distribution based on pairwise interactions. They successfully simulated the regular distribution of $\chi_{chol} = 0.50$, but could not generate other large-scale regular distributions. The Umbrella model implies that the interactions between cholesterol and phospholipid are multibody in nature. The Monte Carlo simulations based on the Umbrella model have successfully simulated a number of cholesterol regular distributions (Huang and Feigenson, 1999; Huang, 2002). In addition, it also makes it possible to analyze the energy requirement for the regular distribution in quantitative terms. In general, to obtain any large stable regular distribution with a perfect long-range order, such as the distributions in Fig. 7, *b*, *d*, or *f*, the critical magnitude of interaction energies needs to be in the order of several kTs (Fig. 8). Thus, it naturally leads to the question of whether or not the cholesterol regular distribution is a common phenomenon in lipid bilayers because the energy requirement is so high. However, our simulation results as demonstrated in Figs. 8 and 9 show that a significant number of small dynamic domains of regular distribution can actually exist even if the magnitude of interactions is many times smaller than the critical values.

Based on a partition measurement, Wang et al. (1998) estimated that, at $\chi_{chol} = 0.50$ in PC, the area of regular

distribution domains can be as high as 80% of the total membrane surface area. Assuming that the percentage of regular area is equivalent to the parameter $N_c(0)/N_c$ in Fig. 8, the value of ΔE_c for 50 mol% cholesterol in PC would be close to 1.3 kT. This indicates that in real lipid membranes, the magnitude of interaction is indeed smaller than the critical value and the observed regular distribution phenomena are caused by dynamic domains.

It is difficult to estimate the lifetime of these dynamic domains in a Monte Carlo simulation, because establishing the correlation between Monte Carlo steps and real time is not a trivial task. However, given the typical time for a lipid to exchange its position with one of its nearest neighbors being $\sim 10^{-7}$ s (Marsh et al., 1982), the lifetime of these dynamic domains should at least be longer than a few microseconds. On the other hand, the fluorescence lifetimes of DHE and DPH-PC in lipid bilayers are much shorter, i.e., in the nanoseconds range (Liu et al., 1997; Cannon et al., 2003). It is therefore reasonable to assume that the changes of fluorescence signal at the regular distribution composition reports the existence of these small dynamic domains. This interpretation of dynamic domain is consistent with the observation that regular distribution measurements are quite sensitive to sample preparation and incubation. Nevertheless, the existence of these dynamic domains does indicate the importance of multibody interaction between cholesterol and phospholipids.

Cholesterol-lipid interaction and Umbrella model

The Umbrella model was originally proposed to explain the solubility limit of cholesterol in lipid bilayers (Huang and Feigenson, 1999). It hypothesizes that the key requirement for cholesterol-phospholipid mixing is that the polar phospholipid headgroups must cover the nonpolar bodies of cholesterol to avoid the unfavorable free energy of cholesterol contact to water. This coverage requirement results in an overall favorable attraction between cholesterol and phospholipids and an unfavorable repulsion between cholesterol. On the other hand, as the cholesterol molecules partially hide under the headgroups of phospholipid, the rigid bodies of cholesterol restrict the motion of phospholipid acyl chains, resulting in a smaller unfavorable free-energy penalty due to the reduction of chain conformation entropy (Huang, 2002). The balance between the large favorable mixing energy and the smaller unfavorable entropy penalty largely regulates the mixing behavior of phospholipid and cholesterol. So far, the Umbrella model has explained and predicted a number of experiment results:

1. Cholesterol solubility in a lipid bilayer. The solubility limit of cholesterol was interpreted as the concentration of cholesterol at which not all cholesterols can be effectively covered by phospholipid headgroups. At the solubility limit, cholesterol chemical potential jumps, leading to its precipitation from the bilayer. Computer simulation based on the Umbrella model showed that cholesterol precipitation is most likely to occur near three discrete values of cholesterol mol fraction, 0.50, 0.57, and 0.67 (Huang and Feigenson, 1999). The model explained the precise values of the observed solubility limits, and that the solubility limit should be higher in a PC bilayer (with large headgroups) than that in a PE bilayer (with small headgroups).
2. Regular distribution at 0.57. The computer simulation also predicted the cholesterol regular distributions at 0.57 and 0.67, which were experimentally verified in this study.
3. Regular distribution at low cholesterol concentration. We have successfully simulated a number of cholesterol regular distributions at low cholesterol concentration ($\chi_{chol} = 0.154, 0.25, 0.40,$ and 0.5). The study revealed that the unfavorable acyl chain multibody interaction due to reduction of conformation entropy is crucial for cholesterol regular distribution at low cholesterol concentration (Huang, 2002). We found that in general, conventional pairwise-additive repulsive forces cannot produce regular distributions. Instead, a multibody (nonpairwise) interaction is required. For the first time, these regular distributions were simulated starting from a reasonable set of microscopic interaction energies.
4. Increase of acyl chain order by cholesterol. Because cholesterol molecules need to squeeze into the acyl chain region and partially hide under the phospholipid headgroups, it will restrict the motions of acyl chains or even force acyl chain to adapt nearly all-*trans* conformations. The acyl chain order parameter should increase (Stockton and Smith, 1976; Vist and Davis, 1990). Recent molecular dynamics simulations showed that cholesterol molecules are covered by DPPC headgroups in a bilayer and conformation of acyl chains next to cholesterol is quite restricted (Smondyrev and Berkowitz, 1999; Tu et al., 1998; Chiu et al., 2001; Cannon et al., 2003).
5. Cholesterol condensing effect. Because cholesterol is partially hiding under the headgroups of phospholipid, the total surface area of the bilayer should be smaller than the sum of the surface area of pure phospholipid bilayer and the total cross-sectional area of cholesterol (Leathes, 1925; Demel et al., 1967).
6. Reduction of membrane permeability. Cholesterol increases the packing density in acyl chain region. The membrane permeability should decrease (Kinsky et al., 1967).
7. Expansion of phospholipid headgroup. As the cholesterol concentration increases, the phospholipid headgroups need to expand and reorient toward the membrane surface to cover more interfacial area per headgroup. This is consistent with earlier findings that PC headgroups become more hydrated when cholesterol was added (Kusumi et al., 1986; Ho et al., 1995). Molecular dynamic simulations have shown that PC headgroup-headgroup distance increases and phospholipids in close contact with cholesterol have a slightly larger average area per

headgroup and their headgroups are oriented nearly parallel to the membrane surface (Pasenkiewicz-Gierula et al., 2000; Smondyrev and Berkowitz, 1999).

Possible mechanism of lipid raft formation

Lipid rafts are cholesterol and sphingolipid-rich lipid domains. The Umbrella model also suggests a possible mechanism of its formation. It has been suggested that by forming a liquid-ordered phase with sphingomyelin, cholesterol increases the attractive van der Waals force with the long saturated acyl chains of sphingomyelin (Harder and Simons, 1997). Others have suggested that rafts are driven by hydrogen bonding between cholesterol and the sphingolipid ceramide backbone (Brown and London, 1998; Simons and Ikonen, 1997). Here we propose an alternative mechanism: raft formation is driven by an entropy effect of hydrocarbon chains. Due to the coverage requirement, cholesterol has a strong tendency to mix well with other lipid molecules containing large polar headgroups, such as phosphatidylcholines and sphingolipids. In a lipid mixture with phosphatidylcholines having unsaturated chains and sphingolipids having more saturated chains, cholesterol can mix well with both lipids, because both can provide the needed coverage for cholesterol. However, association with sphingolipids can be much more favorable than association with phosphatidylcholines for the following two reasons: 1), the unfavorable free energy due to the chain entropy effect will be reduced by the long and saturated sphingolipid hydrocarbon chains having a natural tendency to form straight conformations, even without cholesterol; and 2), phosphatidylcholines with unsaturated hydrocarbon chains will have less room under the headgroups for cholesterol due to the *cis* double bonds. This explanation is consistent with experimental findings that cholesterol has low affinity to unsaturated acyl chains and can selectively form association with saturated chains even in a pure PC bilayer (Mitchell and Litman, 1998; Niu and Litman, 2002). Based on our previous work (Huang, 2002), this entropy effect can be quite large. Thus, it is likely to contribute to lipid raft formation.

This work was supported by the Higher Education Assistance Fund and Petroleum Research Fund grants given to J.H. and the Welch Research Foundation (D-1158) given to K.H.C.

REFERENCES

Brown, D., and E. London. 1998. Functions of lipid rafts in biological membranes. *Ann. Rev. of Cell and Dev. Biol.* 14:111–136.

Brown, D., and E. London. 2000. Structure and function of sphingolipid- and cholesterol-rich membrane rafts. *J. Biol. Chem.* 275:17221–17224.

Buboltz, J. T., and G. W. Feigenson. 1999. A novel strategy for the preparation of liposomes: rapid solvent exchange. *Biochim. Biophys. Acta.* 1417:232–245.

Cannon, B., G. Heath, J. Huang, P. Somerharju, J. A. Virtanen, and K. H. Cheng. 2003. Time-resolved fluorescence and fourier transform infrared spectroscopic investigations of lateral packing defects and superlattice domains in compositionally uniform phosphatidylcholine bilayers. *Biophys. J.* 84:3777–3791.

Chiu, S. W., E. Jakobsson, and H. L. Scott. 2001. Combined Monte Carlo and molecular dynamics simulation of hydrated lipid-cholesterol lipid bilayers at low cholesterol concentration. *Biophys. J.* 80:1104–1114.

Chong, P. L.-G. 1994. Evidence for regular distribution of sterols in liquid crystalline phosphatidylcholine bilayers. *Proc. Natl. Acad. Sci. USA.* 91:10069–10073.

Chong, P. L.-G., and I. P. Sugar. 2002. Fluorescence studies of lipid regular distribution in membranes. *Chem. Phys. Lipids.* 116:153–175.

Chong, P. L.-G., D. Tang, and I. P. Sugar. 1994. Exploration of physical principles underlying lipid regular distribution: effects of pressure, temperature, and radius of curvature on E/M dips in pyrene-labeled PC/DMPC binary mixtures. *Biophys. J.* 66:2029–2038.

Dale, R. E., J. Eisinger, and W. E. Blumberg. 1979. The orientational freedom of molecular probes: the orientation factor in intramolecular energy transfer. *Biophys. J.* 26:161–193.

Demel, R. A., L. L. M. van Deenen, and B. A. Pethica. 1967. Monolayer interactions of phospholipids and cholesterol. *Biochim. Biophys. Acta.* 135:11–19.

Dietrich, C., L. A. Bagatolli, Z. N. Volovyk, N. L. Thompson, M. Levi, K. Jacobson, and E. Gratton. 2001. Lipid rafts reconstituted in model membranes. *Biophys. J.* 80:1417–1428.

Field, K. A., D. Holowka, and B. Baird. 1997. Compartmentalized activation of the high affinity immunoglubulin E receptor within membrane domains. *J. Biol. Chem.* 272:4276–4280.

Finegold, L. (ed.) 1993. Cholesterol in Membrane Models. CRC Press, Boca Raton, FL.

Förster, T. 1948. Intermolecular energy migration and fluorescence. (R. S. Knox, translator, University of Rochester, New York. 1984). *Ann. Physik.* 2:55–75.

Gandhavadi, M., D. Allende, A. Vidal, S. A. Simon, and T. J. McIntosh. 2002. Structure, composition, and peptide binding properties of detergent soluble bailers and detergent resistant rafts. *Biophys. J.* 82:1469–1482.

Gratton, E., D. M. Jameson, and R. D. Hall. 1984. Multifrequency phase and modulation fluorometry. *Annu. Rev. Biophys. Bioeng.* 13:105–124.

Harder, T., and K. Simons. 1997. Caveolae, DIGs, and the dynamics of sphingolipid-cholesterol microdomains. *Curr. Opin. Cell Biol.* 9:534–542.

Ho, C., S. J. Slater, and C. D. Stubbs. 1995. Hydration and order of lipid bilayers. *Biochemistry.* 34:6188–6195.

Huang, J. 2002. Exploration of molecular interactions in cholesterol superlattices: effect of multibody interactions. *Biophys. J.* 83:1014–1025.

Huang, J., J. T. Buboltz, and G. W. Feigenson. 1999. Maximum solubility of cholesterol in phosphatidylcholine and phosphatidylethanolamine bilayers. *Biochim. Biophys. Acta.* 1417:89–100.

Huang, J., and G. W. Feigenson. 1993. Monte Carlo simulation of lipid mixtures: finding phase separation. *Biophys. J.* 65:1788–1794.

Huang, J., and G. W. Feigenson. 1999. A microscopic interaction model of maximum solubility of cholesterol in lipid bilayers. *Biophys. J.* 76:2142–2157.

Ipsen, J. H., G. Karlstrom, O. G. Mouritsen, H. Wennerstrom, and M. J. Zuckermann. 1987. Phase equilibria in the PC-cholesterol system. *Biochim. Biophys. Acta.* 905:162–172.

Kingsley, P. B., and G. W. Feigenson. 1979. The synthesis of a perdeuterated phospholipid:1,2-dimyristoyl-*sn*-glycero-3-phosphocholine-d_{72}. *Chem. Phys. Lipids.* 24:135–147.

Kinsky, S. C., S. A. Luse, D. Zopf, L. L. M. van Deenen, and J. Haxby. 1967. Interaction of filipin and derivatives with erythrocyte membranes and lipid dispersions: electron microscopic observations. *Biochim. Biophys. Acta.* 135:844–861.

Kusumi, A., W. K. Subczynski, M. Pasenkiewicz-Gierula, J. S. Hyde, and H. Merkle. 1986. Spin-label studies of phosphatidylcholine-cholesterol

membranes: effects of alkyl chain length and unsaturation in the fluid phase. *Biochim. Biophys. Acta*. 854:307–317.

Lakowicz, J. R. 1983. Principles of Fluorescence Spectroscopy. Plenum Publishing Co., New York.

Leathes, J. B. 1925. Role of fats in vital phenomena. *Lancet*. 208:853–856.

Li, L. K., L. So, and A. Spector. 1985. Membrane cholesterol and phospholipid in consecutive concentric sections of human lenses. *J. Lipid Res*. 26:600–609.

Li, L. K., L. So, and A. Spector. 1987. Age-dependent changes in the distribution and concentration of human lens cholesterol and phospholipids. *Biochim. Biophys. Acta*. 917:112–120.

Liu, F., I. P. Sugar, and P. L.-G. Chong. 1997. Cholesterol and ergosterol superlattices in three-component liquid crystalline lipid bilayers as revealed by dehydroergosterol fluorescence. *Biophys. J*. 72:2243–2254.

Loomis, C. R., G. G. Shipley, and D. M. Small. 1979. The phase behavior of hydrated cholesterol. *J. Lipid Res*. 20:525–535.

Marsh, D., A. Watts, R. D. Pates, R. Uhl, P. F. Knowles, and M. Esmann. 1982. ESR spin-label studies of lipid-protein interactions in membranes. *Biophys. J*. 37:265–274.

Metropolis, N., A. W. Rosenbluth, M. N. Rosenbluth, and A. Teller. 1953. Equation of state calculations by fast computing machines. *J. Chem. Phys*. 21:1087–1092.

Mitchell, D. C., and B. J. Litman. 1998. Effect of cholesterol on molecular order and dynamics in highly polyunsaturated phospholipid bilayers. *Biophys. J*. 75:896–908.

Mukherjee, S., X. Zha, I. Tabas, and F. R. Maxfield. 1998. Cholesterol distribution in living cells: fluorescence imaging using dehydroergosterol as a fluorescent cholesterol analog. *Biophys. J*. 75:1915–1925.

Niu, S. L., and B. J. Litman. 2002. Determination of membrane cholesterol partition coefficient using a lipid vesicle-cyclodextrin binary system: effect of phospholipid acyl chain unsaturation and headgroup composition. *Biophys. J*. 83:3408–3415.

Pasenkiewicz-Gierula, M., T. Róg, K. Kitamura, and A. Kusumi. 2000. Cholesterol effects on the phosphatidylcholine bilayer polar region: a molecular simulation study. *Biophys. J*. 78:1376–1389.

Samsonov, A. V., I. Mihalyov, and F. S. Cohen. 2001. Characterization of cholesterol-sphingomyelin domains and their dynamics in bilayer membrane. *Biophys. J*. 81:1486–1500.

Schroeder, F., J. R. Jefferson, A. B. Kier, J. Knittel, T. J. Scallen, W. G. Wood, and I. Hapala. 1991. Membrane cholesterol dynamics: cholesterol domains and kinetic pools. *Proc. Soc. Exp. Biol. Med*. 196:235–252.

Simons, K., and E. Ikonen. 1997. Functional rafts in cell membranes. *Nature*. 387:569–572.

Simons, K., and E. Ikonen. 2000. How cells handle cholesterol. *Science*. 290:1721–1726.

Smondyrev, A. M., and M. L. Berkowitz. 1999. Structure of dipalmitoylphosphatidylcholine/cholesterol bilayer at low and high cholesterol concentrations: molecular dynamics simulation. *Biophys. J*. 77:2075–2089.

Somerharju, P., J. A. Virtanen, and K. H. Cheng. 1999. Lateral organization of membrane lipids: the superlattice view. *Biochim. Biophys. Acta*. 1440:32–48.

Stockton, B. W., and I. C. P. Smith. 1976. A deuterium NMR study of the condensing effect of cholesterol on egg phosphatidylcholine bilayer membranes. *Chem. Phys. Lipids*. 17:251–261.

Sugar, I. P., D. Tang, and P. L.-G. Chong. 1994. Monte Carlo simulation of lateral distribution of molecules in a two-component lipid membrane. Effect of long-range repulsive interactions. *J. Phys. Chem*. 98:7201–7210.

Sugar, I. P., T. E. Thompson, K. K. Thompson, and R. L. Biltonen. 1998. Monte Carlo simulation of two-component bilayers: DMPC/DSPC mixtures. *Biophys. J*. 74:373a. (Abstr.)

Tang, D., and P. L.-G. Chong. 1992. E/M dips: Evidence for lipids regularly distributed into hexagonal super-lattices in pyrene-PC/DMPC binary mixtures at specific concentrations. *Biophys. J*. 63:903–910.

Tu, K., M. L. Klein, and D. J. Tobias. 1998. Constant-pressure molecular dynamics investigation of cholesterol effects in a dipalmitoylphosphatidylcholine bilayer. *Biophys. J*. 75:2147–2156.

Virtanen, J. A., M. Ruonala, M. Vauhkonen, and P. Somerharju. 1995. Lateral organization of liquid-crystalline cholesterol-dimyristoylphosphatidylcholine bilayers. Evidence for domains with hexagonal and centered rectangular cholesterol superlattices. *Biochemistry*. 34:11568–11581.

Virtanen, J. A., P. Somerharju, and P. K. J. Kinnunen. 1988. Prediction of patterns for the regular distribution of soluted guest molecules in liquid crystalline phospholipid membranes. *J. Mol. Electron*. 4:233–236.

Vist, M., and J. H. Davis. 1990. Phase equilibria of cholesterol/dipalmitoylphosphatidylcholine mixtures: ^{2}H nuclear magnetic resonance and differential scanning calorimetry. *Biochemistry*. 29:451–464.

Wang, T. Y., R. Leventis, and J. R. Silvius. 2000. Fluorescence-based evaluation of the partitioning of lipids and lipidated peptides into liquid-ordered lipid microdomains: a model for molecular partitioning into lipid rafts. *Biophys. J*. 79:919–933.

Wang, M. M., I. P. Sugar, and P. L.-G. Chong. 1998. Role of the sterol superlattice in the partitioning of the antifungal drug nystatin into lipid membranes. *Biochemistry*. 37:11797–11805.

Wang, M. M., I. P. Sugar, and P. L.-G. Chong. 2002. Effect of double bond position on dehydroergosterol fluorescence intensity dips in phosphatidylcholine bilayers with saturated sn-1 and monenoic sn-2 acyl chains. *J. Phys. Chem*. 106:6338–6345.

Xu, X., and E. London. 2000. The effect of sterol structure on membrane lipid domains reveals how cholesterol can induce lipid domain formation. *Biochemistry*. 39:843–849.